

Adversarial Curiosity

Bernadette Bucher*, Karl Schmeckpeper*, Nikolai Matni, Kostas Daniilidis

GRASP Laboratory, University of Pennsylvania

bucherb, karls, nmatni, kostas@seas.upenn.edu

Abstract: Model-based curiosity combines active learning approaches to optimal sampling with the information gain based incentives for exploration presented in the curiosity literature. Existing model-based curiosity methods look to approximate prediction uncertainty with approaches which struggle to scale to many prediction-planning pipelines used in robotics tasks. We address these scalability issues with an adversarial curiosity method minimizing a score given by a discriminator network. This discriminator is optimized jointly with a prediction model and enables our active learning approach to sample sequences of observations and actions which result in predictions considered the least realistic by the discriminator. We demonstrate increased downstream task performance in simulated environments using our adversarial curiosity approach compared to other model-based and model-free exploration strategies. We further demonstrate the ability of our adversarial curiosity method to scale to a robotic manipulation prediction-planning pipeline where we improve sample efficiency and prediction performance for a domain transfer problem.

Keywords: Active Learning, Curiosity, Discriminator

1 Introduction

Methods for *curiosity* maximize expected information gain of predictive models (typically via informal mathematical proxies) which can be used to perform targeted sampling [1, 2, 3]. Model-free curiosity derives rewards *after* an action is taken and thus requires knowledge of the action outcome. This approach necessitates integration with model-free reinforcement learning in which rewards provide feedback to an updated policy for selecting actions. In contrast, model-based methods are active learning strategies which use a prediction model directly to select actions, so curiosity measurements must be made *before* the action is taken to execute curious behavior. The fundamental difference between these approaches is visualized in Figure 2.

The active learning and active perception literature has long established the ability of good sampling strategies to increase sample efficiency and model performance in robotics [4, 5, 6]. Model-based curiosity research distinguishes itself within this broader set of work by focusing on objectives for predictive model information gain. Current model-based curiosity methods evaluated in simulated environments face scalability issues, limiting the ability of this line of research to contribute

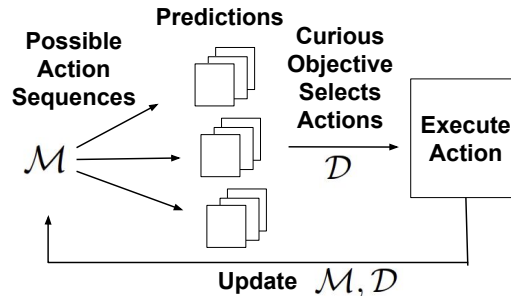


Figure 1: Our approach for model based curiosity. A predictive model generates predictions on a number of potential trajectories. These predictions are evaluated with a discriminator and trajectory that corresponds to the least realistic prediction is executed. The predictive model and the discriminator are updated with the newly collected data.

* Alphabetical ordering; the first two authors contributed equally.

to advancing prediction and planning in real robotics environments and tasks. These challenges are particularly pronounced when predictive models are computed from high dimensional sensory data such as images.

To demonstrate the scalability of our adversarial method, we target a class of robotic manipulation problems with data-driven prediction-planning solutions that are trained with only randomly sampled data in the existing literature. Robot learning methods already face a scalability problem, as large amounts of data are required for training which is time-consuming to collect. To address this challenge, recent research demonstrated the ability of a class of these data-driven methods to transfer across platforms [7]. This capability allows for publicly available datasets to be leveraged for the bulk of the training, and only a small amount of data needs to be collected for fine-tuning in the new domain. We propose performing targeted sampling with our adversarial curiosity objective in the new domain instead of random sampling, as illustrated in Figure 3, in order to further increase the performance and sample efficiency of this robotic manipulation pipeline.

In work most similar to our own, Shyam et al. [8] provides an approach to computing certainty of model predictions before taking the chosen action in a model-based approach to curiosity. This computation is derived from the variance of outcomes computed within an ensemble of prediction models. The action resulting in the highest variance of outcome expectations is taken. This ensemble-based approach provides an elegant approximation of model uncertainty but does not scale to

compute intensive prediction models such as many modern vision-based prediction methods which may each require the full capacity of a GPU to train. Our formulation of model-based curiosity uses an objective based on minimizing a score given by a discriminator network in order to choose actions which result in outcomes considered the least realistic by our adversarial network. Our method integrates with model-based reinforcement learning via a more scalable measurement for curiosity.

Our Contributions We present an adversarial curiosity reward which we use as an objective in model-based reinforcement learning systems. We integrate this method into two distinct prediction-planning pipelines. In the first pipeline, we perform state-based prediction and plan with a Markov Decision Process to generate exploration and exploitation policies. This pipeline is compatible with existing model-based curiosity methods against which we compare our approach in simulated task execution. We then scale our method to a practical robotics manipulation problem, integrating our discriminator with a video prediction model and the cross-entropy method for planning. Our method improved sample efficiency without sacrificing task performance. In addition, our method increased prediction performance. To the best of our knowledge, this application is the first use of model-based curiosity for vision-based robotic manipulation.

Our paper is organized as follows. First, we review the literature on sampling with both curiosity and active learning methods. Then, we present our adversarial curiosity objective for sampling in a model-based reinforcement learning problem. Next, we favorably compare the ability of our method to complete downstream tasks with other curiosity methods in simulation using policies learned via exploration. Finally, we demonstrate the ability of our method to scale to a robotic manipulation pipeline in which we show increased sample efficiency and improved prediction performance in a domain transfer problem.

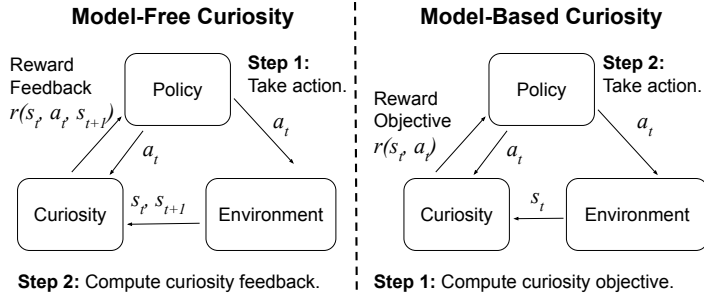


Figure 2: Our model-based curiosity approach contrasted to established model-free formulations of curiosity. Existing model-free approaches to curiosity calculate the curiosity score after the action has been taken, while our approach uses the curiosity score to decide which action to take.

2 Related Work

We specify our method as an adversarial curiosity objective which we use to perform active learning in model-based reinforcement learning. Thus, we contextualize our work in the active learning and curiosity literature. The goal of both active learning and curiosity is to provide a method for selecting samples with which to train a model such that the model gains the most possible information from the sampled data.

Model-Free Curiosity Several existing models use exploration incentives to estimate and seek visual novelty in model-free reinforcement learning. Approaches include generalizing count-based exploration to continuous domains [10, 11], rewarding the policy based on the observed error in a prediction model [12, 13, 14], rewarding the policy based on the disagreement in an ensemble [15, 16], and rewarding the policy based on information gain in a Bayesian neural network [17]. We present a model-based curiosity method using the scores from a discriminator network. These same scores could be used as feedback to a model-free method, but we only evaluate the model-based case in this work to highlight the key characteristic of our curiosity approach: scalability.

Model-Based Curiosity There are far fewer model-based curiosity methods than model-free. Discrete count-based methods [18] estimate the learning progress of a potential sample [19]. Shyam et al. [8], Sekar et al. [20] use ensembles of models to estimate uncertainty in predictions. Bechtle et al. [21] minimizes the uncertainty of Bayesian models. Our work differs from previous model-based active exploration methods in that it is able to operate computationally efficiently in high-dimensional continuous domains through the use of a discriminator which provides scores for the realism of our model predictions.

Adversarial Curiosity The concept of adversarial curiosity was first proposed by Schmidhuber [22] prior to the integration of curiosity with planning algorithms. This work suggested that the formulation of the minimax problem presented a method of encoding introspective behavior in a model. Schmidhuber [23] further argues that minimax optimization problems such as the one we propose here provide intrinsic motivation for a model to invent novel information about which to learn. This behavioral paradigm is considered a form of curiosity [1, 22, 23, 3]. We propose the first explicit model of adversarial curiosity with experimental evaluation in this work.

Active Learning Active learning is the process where a machine learning algorithm selects its training data to improve its data efficiency and performance [24]. Many methodological approaches to active learning have been proposed, including sampling the most uncertain data points [25, 26, 27], sampling where an ensemble of models disagrees [28, 29, 30], sampling data that will cause the largest expected information gain [31], sampling data that will cause the largest expected change in the model [32, 33, 34], sampling data that will cause the largest expected reduction in variance [5], and sampling data that will cause the largest estimated error reduction [4, 35, 36]. Our approach is most similar to the works that sample the most uncertain data points. To distinguish active learning from curiosity, active learning is specifically formulated to determine samples to select *before* sampling whereas the curiosity literature includes both active methods [21] and methods in which rewards can only be computed *after* sampling [16, 12]. Thus, the method we propose in this work is both a method for curiosity and active learning.

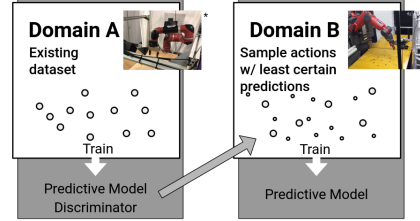


Figure 3: Active sampling to enable domain transfer. In our robotics experiments, our method trains an action-conditioned prediction model and a discriminator on the dataset in the initial domain. It then samples actions from the new domain that result in the most uncertain predictions, allowing it to train a prediction model in the new domain with a small number of samples.

*Image used with permission from [9]

3 Adversarial Curiosity Objective

Consider the dynamics of a system \mathcal{F} mapping past states s_t and actions a_t to future states via

$$s_{t+1:t+T_f+1} = \mathcal{F}(s_{t-T_p:t}, a_{t:t+T_f}), \quad (1)$$

for $T_f, T_p > 0$ future and past time intervals, respectively. We then denote by

$$\mathbf{x} = (s_{t-T_p:t}, a_{t:t+T_f}, s_{t+1:t+T_f+1}) \quad (2)$$

any trajectory generated by system (1), and denote by $p(\mathbf{x})$ the distribution over these trajectories.

Our model-based curiosity method is defined in terms of the following three components:

- i) A model \mathcal{M} generates predictions of future states \hat{s} given past states s and actions a . These predictions are made over a prediction horizon H using a set number of past context states C . Thus, our prediction model is given by

$$\hat{s}_{t+1:t+H+1} = \mathcal{M}(s_{t-C:t}, a_{t:t+H}). \quad (3)$$

To lighten notational burden going forward, we let $\mathbf{a} := a_{t:t+H}$, $\mathbf{c} := s_{t-C:t}$.

- ii) A discriminator \mathcal{D} , which assigns a score d_t to each real trajectory \mathbf{x} generated by system (1) as well as imagined trajectories generated by the prediction model (3). To train the discriminator \mathcal{D} , we solve the minimax optimization problem

$$\min_{\mathcal{M}} \max_{\mathcal{D}} \mathbb{E}_{\mathbf{x} \sim p(\mathbf{x})} [\log \mathcal{D}(\mathbf{x})] + \mathbb{E}_{(\mathbf{c}, \mathbf{a}) \sim p(\mathbf{x})} [\log (1 - \mathcal{D}(\mathbf{c}, \mathbf{a}, \mathcal{M}(\mathbf{c}, \mathbf{a})))] \quad (4)$$

The first term in the objective function of optimization problem (4) captures the ability of the discriminator to identify realistic trajectories generated by system (1), whereas the second term simultaneously reflects the predictive ability of the model \mathcal{M} , as well as the ability of the discriminator \mathcal{D} to distinguish between real and imagined trajectories.

The inner maximization trains the discriminator \mathcal{D} to differentiate between trajectories sampled from the data distribution \mathbf{x} and predicted trajectories $(\mathbf{c}, \mathbf{a}, \mathcal{M}(\mathbf{c}, \mathbf{a}))$. The outer minimization optimizes the performance of the prediction model \mathcal{M} . In summary, this minimax problem sets up a competition in which the prediction model tries to learn to make good enough predictions to fool the discriminator while the discriminator tries to improve differentiation of predictions from data samples.

After \mathcal{D} is trained, the discriminator scores for our imagined trajectories are evaluated as

$$d_t = \mathcal{D}(\mathbf{c}, \mathbf{a}, \mathcal{M}(\mathbf{c}, \mathbf{a})). \quad (5)$$

- iii) With these pieces in place, we can now define the curiosity based optimization problem that we solve in order to select action sequences which optimize a curiosity objective defined in terms of the discriminator score. In particular, we define a planner \mathcal{P} that selects actions which minimize the discriminator score by solving the optimization problem:

$$\mathcal{P}(\mathbf{c}, \mathbf{a}, \mathcal{M}, \mathcal{D}) := \arg \min_{\mathbf{a}} \mathcal{D}(\mathbf{c}, \mathbf{a}, \mathcal{M}(\mathbf{c}, \mathbf{a})) \quad (6)$$

It then follows that the actions resulting in the least realistic predictions are selected by the planner defined by optimization problem (6), resulting in qualitatively more *curious* behavior.

We note that in the domain transfer problem visualized in Figure 3 introduces a variant on this process for sampling. The model \mathcal{M} is first trained jointly with the discriminator \mathcal{D} on data from Domain A. Then, the model \mathcal{M} and the discriminator \mathcal{D} are used in the planner \mathcal{P} to execute the sampling procedure in Domain B in order to gather data for updating \mathcal{M} . If the discriminator will continue to be used for future collection tasks, \mathcal{D} can be trained jointly with \mathcal{M} again to be updated using the newly sampled data. This sampling procedure for domain transfer is laid out in more detail for our specific experimental application in Figure 5.

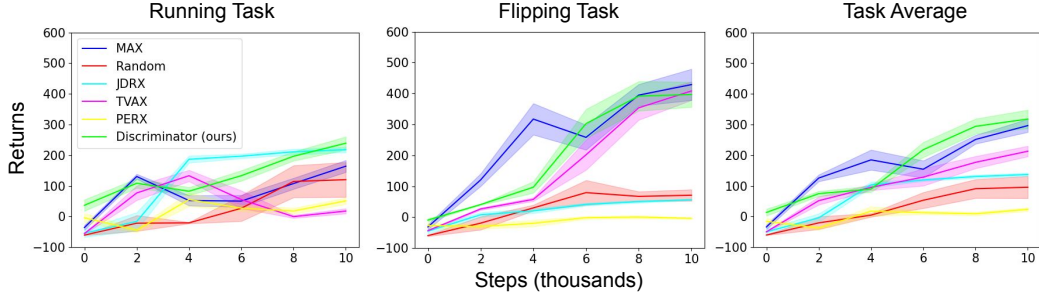


Figure 4: Extrinsic rewards from running and flipping task completion in the Half Cheetah OpenAI environment averaged over 5 trials initiated with random seeds broken down by each distinct method for exploration used in training. Our approach outperforms competing curiosity methods.

4 Exploration Impact on Task Execution

We compare our curiosity method to two model-based exploration methods both presented in [8], the closest work to our own. Model-based active exploration (MAX) rewards exploration with the Jensen-Shannon or Jensen-Rényi divergence between an ensemble of prediction models to measure prediction uncertainty. The Jensen-Rényi divergence is used for continuous state spaces as is the case in our experiments. Trajectory variance active exploration (TVAX) computes the variance in sampled trajectories between an ensemble of prediction models as an exploration reward. We also compare our method to the model-free prediction error approach presented in [12] (PERX) and a model-free version of MAX (JDRX) as well as to random exploration.

In order to compare as fairly as possible to these baselines, we replicate a key experiment from the original presentation of the MAX method using their published hyperparameters. We use the same prediction-planning pipeline proposed with the MAX algorithm so that performance differences can be based solely on the different exploration policy approaches. All methods use an ensemble of fully connected neural networks trained with a negative log-likelihood loss to predict next state distributions. Next state predictions are given by the distribution mean. We emphasize that this use of ensembles as a predictive model is not necessary in the case of our curiosity method other than to standardize the prediction approach in this experiment for comparison purposes whereas MAX, JDRX, and TVAX all require an ensemble-based prediction approach to derive their curiosity rewards. The model-free methods use soft-actor critic (SAC) [37] to learn a policy. The model-based methods are trained with data gathered by an MDP using an exploration objective following the framework presented in [8].

We execute our experiments in the OpenAI Half Cheetah environment which has an 18-dimensional continuous observation space and a 6-dimensional continuous action space [38]. Following [8], we add Gaussian noise of $\mathcal{N}(0, 0.02)$ to the actions to increase the difficulty. Policies are trained purely with each exploration strategy and then used to execute downstream tasks. We compare the performance of each exploration method by evaluating achieved extrinsic rewards in these tasks over 5 randomly seeded trials and present them in Figure 4. We find that our method either outperforms or performs comparably to all the baselines in both downstream tasks: running and flipping.

While we show favorable performance against baseline methods in this frequently used simulation environment, we note that the key contribution of our approach comes from the scalability of the discriminator. Each of the baseline exploration methods presented here is either only compatible with model-free reinforcement learning or relies on the use of ensembles of prediction models to estimate uncertainty. Ensemble-based exploration approaches are not scalable to many more computationally intensive prediction methods such as vision models used in practical robotics tasks, and model-free reinforcement learning faces sample complexity challenges preventing widespread use in robotics. In the remainder of our paper, we demonstrate the ability of our exploration method to scale

effectively to robotics tasks through integration with an established prediction-planning pipeline for manipulation.

5 Robotic Manipulation

We demonstrate the ability of our adversarial curiosity method to meaningfully scale to robotics problems by integrating our approach in a prediction-planning pipeline commonly studied robot learning approaches to manipulation. We demonstrate increased sample efficiency and gains in prediction performance from incorporating our discriminator in this pipeline.

States (denoted s_t in prior sections) are RGB images in this set of experiments, so we specify our notation by referencing these image states as I_t . We use a variant of the prediction model from Dasari et al. [7]. A stack of convolutional LSTMs is used to predict a flow field from an image I_t and action a_t . This flow field is then applied directly to the input image I_t to predict the next image frame \hat{I}_{t+1} . The true next image frame I_{t+1} is observed after the given action is taken.

This network is optimized with an L_1 loss between the predicted image \hat{I}_{t+1} and true image I_{t+1} . In practice, these models perform predictions out to some horizon H using a context of C image frames in which the flow field estimates are applied recursively across the prediction horizon.

We extend the notation presented in Section 3 by setting

$$\mathbf{h} = I_{t+1:t+H+1} \quad (7)$$

such that a sampled trajectory is given by

$$\mathbf{x} = (\mathbf{c}, \mathbf{a}, \mathbf{h}) = (I_{t-C:t}, a_{t+1:t+H+1}, I_{t+1:t+H+1}). \quad (8)$$

In the training procedure described by Step 1 in Figure 5, our prediction model is optimized jointly with the discriminator defined in Section 3. The optimization problem solved by our model \mathcal{M} during training is

$$\begin{aligned} \min_{\mathcal{M}} \max_{\mathcal{D}} \mathbb{E}_{\mathbf{x} \sim p(\mathbf{x})} [L_1(\mathbf{h}, \mathcal{M}(\mathbf{c}, \mathbf{a}))] + \mathbb{E}_{\mathbf{x} \sim p(\mathbf{x})} [\log \mathcal{D}(\mathbf{x})] \\ + \mathbb{E}_{(\mathbf{c}, \mathbf{a}) \sim p(\mathbf{x})} [\log (1 - \mathcal{D}(\mathbf{c}, \mathbf{a}, \mathcal{M}(\mathbf{c}, \mathbf{a})))] \end{aligned} \quad (9)$$

which combines the adversarial minimax game from equation (4) with the L_1 loss on prediction error. This is similar to the loss in [39], where the combination of prediction error and an adversarial loss were shown to improve prediction quality and convergence.

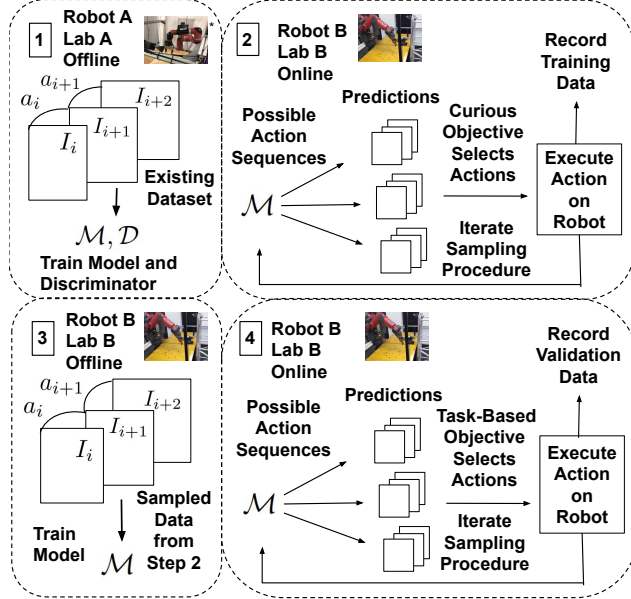


Figure 5: The process used for online training with a curiosity objective provided by the loss from our discriminator network in a domain transfer problem. The model and the discriminator are initially trained on an existing dataset from domain A (1). The model and discriminator are used to select and execute sequences of actions that optimize the curiosity objective in domain B, generating a new dataset (2). The dataset from domain B is used to train the model (3). The model is used to select sequences of actions that optimize a task-based objective, allowing the robot to perform useful tasks in domain B (4).

We use this prediction model and the cross-entropy method (CEM) [40] to optimize for a sequence of actions that minimize Equation 6. This procedure causes the robot to select a sequence of actions that generate unrealistic looking predictions.

5.1 Sampling Analysis

We evaluate the ability of our curiosity objective to effectively explore the environment by comparing the behavior of our curious policy to the behavior of the random policy used in prior work. To make this comparison, we execute Steps 1 and 2 visualized in Figure 5. First, our prediction model and discriminator is jointly trained on Sawyer data from the RoboNet dataset [7] by optimizing equation (9). Then, we use each policy to separately sample trajectories on a Baxter robot platform. Our curious policy was able to visit a more diverse array of states and grasp more objects than the existing random policy.

Our policy is able to significantly increase the quantity of objects that the robot grasps. Since the interaction between the robot and objects are some of the most difficult things to predict in the tabletop manipulation setting, having more data about robot-object interactions makes a collected dataset more effective in training prediction models. Figure 7 shows a histogram of when the grippers of the robot experienced non-zero forces during data collection for both the curious and the random policies. Non-zero forces indicate that an object is between the grippers, preventing them from fully closing. When following the curious policy, the robot spends a larger portion of its time grasping objects. Examples of trajectories collected by our curious policy are provided in the appendix.

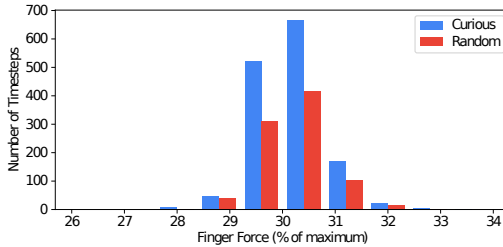


Figure 7: Histograms of the non-zero gripper forces experienced while executing each policy. Each policy was executed for 650 trajectories of 30 timesteps. Non-zero force occurs when a large enough object is grasped by the robot’s fingers. The curious policy spends significantly more time grasping objects than the random policy.

The samples collected with our curious policy enable statistically significant prediction improvement on control tasks over samples collected with our random policy. The L_2 error improvement for the model trained with the data collected with the curious policy at different numbers of samples is visualized in Figure 8b. Error improvement for the curious policy is especially pronounced at lower numbers of samples. Qualitative prediction results are shown in Figure 8a. The model trained with the curious data more accurately

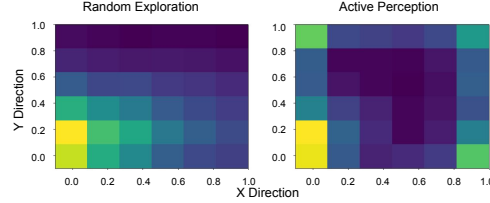
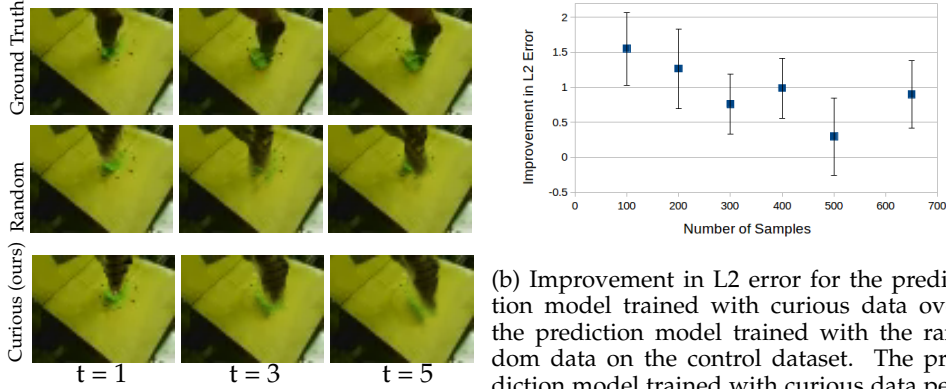


Figure 6: Heat map of the state space regions explored by each policy over 650 trajectories. Regions which are more yellow indicate a higher count for the end effector of the Baxter arm accessing that discretized x-y region. Our curious model explores all corners of the state space, focusing on the edges where objects accumulate, while the random exploration remains near its starting location.

Our curious policy also explores a different distribution of robot states. Figure 6 shows a heatmap of the amount of time the robot’s end effector spends at each location in the xy-plane. The curious policy explores more interesting regions of the state space, such as edges of the bins. The walls of the bin are interesting because they block the motion of objects, causing the objects to have more complicated dynamics than when they are in the center of the bin.

5.2 Control and Prediction Performance

We also evaluated the ability of the model trained with data collected under different policies to perform prediction and robotic control by executing Steps 3 and 4 visualized in Figure 5.



(a) Example predictions on the control dataset. All models were trained with 650 samples. In the model trained with the curious data, the object becomes more blurry, but its motion is much more accurate.

(b) Improvement in L2 error for the prediction model trained with curious data over the prediction model trained with the random data on the control dataset. The prediction model trained with curious data performs better by more than the standard error on all but one quantity of samples. The improved performance is particularly pronounced when lower numbers of samples are used in training.

Figure 8: Qualitative and quantitative prediction results in the robotic environment.

tracks the position of the object. Additional details regarding our prediction results are provided in the appendix.

| | Curious | Random |
|-----------------------|------------------|------------------|
| Avg Dist to Goal (cm) | 9.75 ± 1.10 | 8.59 ± 1.09 |
| Success (%) | 34.38 ± 8.53 | 37.50 ± 8.70 |

Table 1: Mean and standard error of change in object distance from goal and successful completion of the manipulation from 32 Baxter pushing trials using each model (curious and random). Successful completion of the manipulation task is considered object overlap with the physical marked goal (not overlap with the goal marked in pixel space). Results from each approach are comparable.

performed the control experiments with the models trained with 650 samples, which has one of the smallest improvements in prediction error between the models trained with curious and random samples. In future work, we intend to investigate the relationship between prediction and control performance in our experiments.

6 Conclusion

We presented an adversarial curiosity approach which we use to actively sample data used to train a prediction model. Our method optimizes an objective given by the score from a discriminator network to choose the sequence of actions that corresponds to the least realistic sequence of predicted observations. We favorably compared our approach in simulated task execution to existing model-based curiosity methods. We show the generality of our approach by integrating it with two different prediction and planning pipelines. We then demonstrated the key capability of our model-based curiosity approach to scale to a practical robotic manipulation problem where we demonstrate increased sample efficiency and improved prediction performance in a domain transfer problem. In future work, we plan to expand our research into effective ways to improve manipulation task performance for robotic learning pipelines through the use of active exploration methods.

Acknowledgments

The authors are grateful for support through the Curious Minded Machines project funded by the Honda Research Institute.

References

- [1] J. Schmidhuber. Formal theory of creativity, fun, and intrinsic motivation (1990;2013;2010). IEEE Trans. on Auton. Ment. Dev., 2(3):230–247, 2010.
- [2] J. Schmidhuber. A possibility for implementing curiosity and boredom in model-building neural controllers. In Proc. of the First Int. Conf. on Simul. of Adaptive Behavior, 1990.
- [3] A. Jaegle, V. Mehrpour, and N. Rust. Visual novelty, curiosity, and intrinsic reward in machine learning and the brain. arXiv preprint arXiv:1901.02478, 2019.
- [4] N. Roy and A. McCallum. Toward optimal active learning through sampling estimation of error reduction. ICML, 2001.
- [5] D. A. Cohn, Z. Ghahramani, and M. I. Jordan. Active learning with statistical models. NIPS, 1996.
- [6] R. Bajcsy and M. Campos. Active and exploratory perception. CVGIP: Image Understanding, 56(1):31–40, 1992.
- [7] S. Dasari, et al. Robonet: Large-scale multi-robot learning. CoRL, 2019.
- [8] P. Shyam, W. Jaśkowski, and F. Gomez. Model-based active exploration. ICML, 2019.
- [9] A. Xie, et al. Improvisation through Physical Understanding: Using Novel Objects as Tools with Visual Foresight. RSS, 2019.
- [10] M. Bellemare, et al. Unifying count-based exploration and intrinsic motivation. NIPS, 2016.
- [11] G. Ostrovski, et al. Count-based exploration with neural density models. ICML, 2017.
- [12] D. Pathak, et al. Curiosity-driven exploration by self-supervised prediction. CVPR, 2017.
- [13] Y. Burda, et al. Exploration by random network distillation. arXiv preprint arXiv:1810.12894, 2018.
- [14] B. Bucher, et al. Perception-driven curiosity with bayesian surprise. RSS Workshop on Combining Learning and Reasoning for Human-Level Robot Intelligence, 2019.
- [15] I. Osband, et al. Deep exploration via bootstrapped dqn. NIPS, 2016.
- [16] D. Pathak, D. Gandhi, and A. Gupta. Self-Supervised Exploration via Disagreement. ICML, 2019.
- [17] R. Houthoofd, et al. Vime: Variational information maximizing exploration. NIPS, 2016.
- [18] M. Kearns and S. Singh. Near-optimal reinforcement learning in polynomial time. Machine Learning, 49(2-3):209–232, 2002.
- [19] M. Lopes, et al. Exploration in model-based reinforcement learning by empirically estimating learning progress. NIPS, 2012.
- [20] R. Sekar, et al. Planning to explore via self-supervised world models. ICML, 2020.
- [21] S. Bechtle, et al. Curious ilqr: Resolving uncertainty in model-based rl. ICML Workshop on RL4RealLife, 2019.

- [22] J. Schmidhuber. Making the world differentiable: On using self-supervised fully recurrent neural networks for dynamic reinforcement learning and planning in non-stationary environments. Technical report, 1990.
- [23] J. Schmidhuber. Unsupervised minimax: Adversarial curiosity, generative adversarial networks, and predictability minimization. CoRR, abs/1906.04493, 2019.
- [24] B. Settles. Active learning literature survey. Computer Sciences Technical Report 1648, University of Wisconsin–Madison, 2009.
- [25] D. D. Lewis and W. A. Gale. A sequential algorithm for training text classifiers. SIGIR, 1994.
- [26] A. J. Joshi, F. Porikli, and N. Papanikolopoulos. Multi-class active learning for image classification. CVPR, 2009.
- [27] Y. Yang, et al. Multi-class active learning by uncertainty sampling with diversity maximization. IJCV, 113(2):113–127, 2015.
- [28] H. S. Seung, M. Opper, and H. Sompolinsky. Query by committee. COLT, 1992.
- [29] D. Cohn, L. Atlas, and R. Ladner. Improving Generalization with Active Learning. Machine Learning, 15(2):201–221, 1994.
- [30] P. Melville and R. J. Mooney. Diverse ensembles for active learning. ICML, 2004.
- [31] N. Houlsby, et al. Bayesian active learning for classification and preference learning. arXiv preprint arXiv:1112.5745, 2011.
- [32] B. Settles, M. Craven, and S. Ray. Multiple-instance active learning. NIPS, 2008.
- [33] R. Sznitman and B. Jedynak. Active testing for face detection and localization. IEEE Trans. on Pattern Analysis and Machine Intelligence, 32(10):1914–1920, 2010.
- [34] A. Vezhnevets, V. Ferrari, and J. M. Buhmann. Weakly supervised structured output learning for semantic segmentation. CVPR, 2012.
- [35] R. Moskovitch, et al. Improving the detection of unknown computer worms activity using active learning. AAAI, 2007.
- [36] K. Konyushkova, R. Sznitman, and P. Fua. Learning active learning from data. NIPS, 2017.
- [37] T. Haarnoja, et al. Soft actor-critic: Off-policy maximum entropy deep reinforcement learning with a stochastic actor. arXiv preprint arXiv:1801.01290, 2018.
- [38] G. Brockman, et al. Openai gym. arXiv preprint arXiv:1606.01540, 2016.
- [39] A. X. Lee, et al. Stochastic Adversarial Video Prediction. arXiv preprint, apr 2018.
- [40] R. Rubinstein. The Cross-Entropy Method for Combinatorial and Continuous Optimization. Methodology And Computing In Applied Probability, 1(2):127–190, 1999.
- [41] C. Finn and S. Levine. Deep Visual Foresight for Planning Robot Motion. ICRA, 2017.
- [42] R. Zhang, et al. The unreasonable effectiveness of deep features as a perceptual metric. In CVPR, 2018.
- [43] D. P. Kingma and J. Ba. Adam: A Method for Stochastic Optimization. ICLR, 2015.

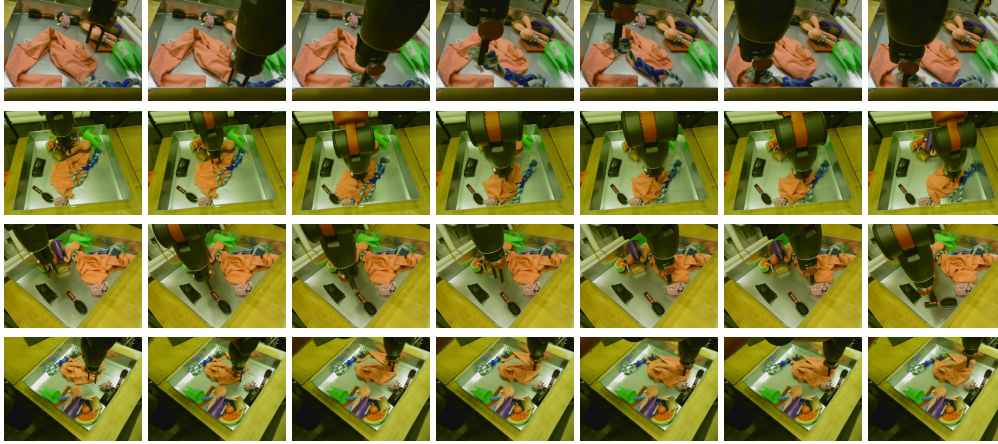


Figure 9: Examples of images from trajectories sampled by the curious data collection policy, showing each of the four camera viewpoints that we collected data from. The selection of objects was held constant throughout all of the data collection including both the curious and random action sampling. Our exploration policy is able to successfully grasp and move objects, though it struggles with grasping the smaller objects such as the hairbrush.

| Method, Number of Samples | L_1 (\downarrow) | L_2 (\downarrow) | PSNR (\uparrow) | SSIM (\uparrow) | LPIPS [42] (\downarrow) |
|-----------------------------|---|--------------------------------------|--------------------------------------|---------------------------------------|---|
| Random, 100 Samples | 0.002789 ± 0.000199 | 20.245 ± 1.085 | 24.263 ± 0.468 | 0.8380 ± 0.0112 | 0.05633 ± 0.00482 |
| Curious (ours), 100 Samples | 0.002611 ± 0.000164 | 18.692 ± 0.863 | 24.746 ± 0.393 | 0.8474 ± 0.0098 | 0.05078 ± 0.00383 |
| Random, 200 Samples | 0.002748 ± 0.000196 | 19.987 ± 1.084 | 24.347 ± 0.453 | 0.8388 ± 0.0111 | 0.05477 ± 0.00462 |
| Curious (ours), 200 Samples | 0.002597 ± 0.000159 | 18.719 ± 0.811 | 24.66 ± 0.363 | 0.8480 ± 0.0093 | 0.05357 ± 0.00385 |
| Random, 300 Samples | 0.00272 ± 0.000189 | 19.708 ± 1.043 | 24.476 ± 0.461 | 0.8403 ± 0.011 | 0.05614 ± 0.00472 |
| Curious (ours), 300 Samples | 0.002642 ± 0.00017 | 18.948 ± 0.905 | 24.664 ± 0.407 | 0.8467 ± 0.0097 | 0.05484 ± 0.00424 |
| Random, 400 Samples | 0.002741 ± 0.00019 | 19.722 ± 1.034 | 24.421 ± 0.441 | 0.8395 ± 0.0107 | 0.05764 ± 0.00449 |
| Curious (ours), 400 Samples | 0.002605 ± 0.000169 | 18.734 ± 0.903 | 24.741 ± 0.394 | 0.8476 ± 0.0096 | 0.05453 ± 0.00404 |
| Random, 500 Samples | 0.002621 ± 0.000177 | 18.888 ± 0.997 | 24.822 ± 0.451 | 0.8468 ± 0.01 | 0.05908 ± 0.00429 |
| Curious (ours), 500 Samples | 0.002592 ± 0.000164 | 18.591 ± 0.854 | 24.795 ± 0.394 | 0.8493 ± 0.0097 | 0.05139 ± 0.00388 |
| Random, 650 Samples | 0.002554 ± 0.000173 | 18.524 ± 0.981 | 24.997 ± 0.454 | 0.8487 ± 0.01 | 0.05910 ± 0.00389 |
| Curious (ours), 650 Samples | 0.002475 ± 0.000147 | 17.625 ± 0.716 | 25.134 ± 0.344 | 0.8537 ± 0.0088 | 0.05265 ± 0.00344 |

Table 2: Means and standard errors for action-conditioned prediction using models trained with various numbers of samples selected from either the curious or random policies.

A Control Experiment Details

For our presented robotics experiments, we execute two rounds of tasks on our Baxter robot platform: one round using the model trained with the curious policy and one round using the random policy. Control experiments are executed by specifying a start location pixel on an object and a goal pixel in image space as visualized in Figure 10. The workspace for both the training data and control experiments is setup with a ring of cameras around the state space in which the robot can act. While the prediction model is trained with data from all viewpoints, only one viewpoint at a time is used to execute the control tasks*. Thus, to account for performance bias between cameras, every manipulation task is executed from each camera using each trained model.

Furthermore, objects are moved in a ring specified around a constant start location to ensure validation is performed for a representative distribution of motions as represented by the marked ring around the shovel

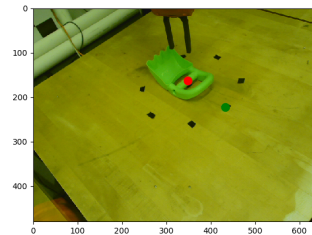


Figure 10: Goal specification for robot manipulation tasks. The robot attempts to move the object at the red dot to the location of the green dot.

*Dasari et al. [7] showed that training prediction models with all viewpoints improves performance over training with a single viewpoint in control executed with a single viewpoint.

| Hyperparameter | Value |
|-------------------------------------|-------|
| Trajectory length | 10 |
| Robot actions per planning interval | 10 |
| CEM iterations | 3 |
| CEM candidate actions per iteration | 600 |
| CEM selection fraction | 0.05 |

Table 4: Hyperparameter values for the planner during task execution

in Figure 10. The object used in the dataset was not included as part of any training data. We completed 64 manipulation tasks on our Baxter robot platform.

B Additional Prediction Results

Figure 11 shows the L_2 error on various samples for models trained with data collected under curious or random policies. By averaging the L_2 error of both models on a given sample, we were able to approximate the difficulty of predicting a given trajectory. Both models give similar qualities of predictions on the easier trajectories, but the model trained with data collected by the curious policy performs noticeably better on the more difficult trajectories. This analysis shows the advantage of our curiosity formulation which explicitly seeks out the most difficult data points to sample and provides an explanation for the source of increased sample efficiency in achieving higher overall prediction performance.

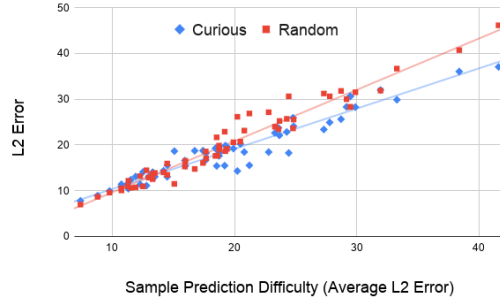


Figure 11: L_2 error of the prediction model trained with curious data compared to the model trained with random data. Both models were trained with 100 samples. The model trained with curious data performs better on harder data points.

We provide samples of the data collected by our curious policy in Figure 9. We list validation results for different numbers of samples across different error metrics in Table 2.

C Experimental Details

Additional visualizations of our results are available on our website at <https://sites.google.com/view/action-for-better-prediction>. Code to reproduce our results in simulation is available at <https://github.com/bucherb/adversarial-curiosity> with all hyperparameters clearly specified in the repository.

| Hyperparameter | Value |
|-------------------------------------|-------|
| Trajectory length | 30 |
| Robot actions per planning interval | 10 |
| CEM iterations | 3 |
| CEM candidate actions per iteration | 200 |
| CEM selection fraction | 0.05 |

Table 3: Hyperparameter values for the planner during exploration

For our robotics results, the hyperparameters for our planner are shown in Table 3 and 4. The hyperparameters for our prediction model used in the robotics experiments are shown in Table 5. We note that since our video prediction model only runs on a single camera’s video stream, and our data collection setup had multiple cameras, our algorithm for curious data collection rotated which camera it was using to plan after every trajectory.

| Hyperparameter | Value |
|----------------------------------|---------------------|
| Schedule sampling k | 4000 |
| Context Frames | 5 |
| Encoder Filters | [128, 256, 256] |
| LSTM Filters | 256 |
| Decoder Filters | 256 |
| Discriminator Kernel size | [3, 4, 4] |
| Discriminator nonlinearity | Leaky ReLU |
| Discriminator Filters | [64, 128, 256, 256] |
| Discriminator training threshold | 0.75 |
| GAN weight | 0.001 |
| L1 weight | 1.0 |
| Optimizer | Adam [43] |
| Learning rate | 0.0001 |
| Beta1 | 0.9 |
| Beta2 | 0.999 |

Table 5: Prediction model hyperparameter values.